HHS Public Access

Author manuscript

Bioelectrochemistry. Author manuscript; available in PMC 2023 April 01.

Published in final edited form as:

Bioelectrochemistry. 2022 April ; 144: 108001. doi:10.1016/j.bioelechem.2021.108001.

High-frequency Irreversible Electroporation Brain Tumor Ablation: Exploring the Dynamics of Cell Death and Recovery

Kelsey R. Murphy[a,*], **Kenneth N. Aycock**[b], **Alayna N. Hay**[c], **John H. Rossmeisl**[c], **Rafael V. Davalos**[b,d], **Nikolaos G. Dervisis**[c,e]

[a]Department of Biomedical and Veterinary Sciences, Virginia-Maryland College of Veterinary Medicine, Blacksburg, Virginia, 24061, United States

[b]Department of Biomedical Engineering and Mechanics, Virginia Polytechnic Institute and State University, Blacksburg, Virginia, 24061, United States

[c]Department of Small Animal Clinical Sciences, Virginia-Maryland College of Veterinary Medicine, Blacksburg, Virginia, 24061, United States

[d]ICTAS Center for Engineered Health, Virginia Tech, Kelly Hall, Blacksburg, VA 24061

[e]Department of Internal Medicine, Virginia Tech Carilion School of Medicine, Roanoke, VA 24016

Abstract

Improved therapeutics for malignant brain tumors are urgently needed. High-frequency irreversible electroporation (H-FIRE) is a minimally invasive, nonthermal tissue ablation technique, which utilizes high-frequency, bipolar electric pulses to precisely kill tumor cells. The mechanisms of H-FIRE-induced tumor cell death and potential for cellular recovery are incompletely characterized. We hypothesized that tumor cells treated with specific H-FIRE electric field doses can survive and retain proliferative capacity. F98 glioma and LL/2 Lewis lung carcinoma cell suspensions were treated with H-FIRE to model primary and metastatic brain cancer, respectively. Cell membrane permeability, apoptosis, metabolic viability, and proliferative capacity were temporally measured using exclusion dyes, condensed chromatin staining, WST-8 fluorescence, and clonogenic assays, respectively. Both tumor cell lines exhibited dose-dependent permeabilization, with 1,500 V/cm permitting and 3,000 V/cm inhibiting membrane recovery 24 hours post-treatment. Cells treated with 1,500 V/cm demonstrated significant and progressive recovery of apoptosis and metabolic activity, in contrast to cells treated with higher H-FIRE doses. Cancer cells treated with recovery-permitting doses of H-FIRE maintained while those treated with recovery-inhibiting doses lost proliferative capacity. Taken together, our data suggest that H-FIRE induces reversible and irreversible cellular damage in a dose-dependent manner, and the presence of dose-dependent recovery mechanisms permits tumor cell proliferation.

[*]Correspondence: krmurphy96@vt.edu; Tel.: (+1 6035215555).

Declaration of Competing Interest

Davalos, Aycock, Dervisis, and Rossmeisl have pending and issued patents related to electroporation.

Keywords

high-frequency irreversible electroporation; brain cancer; cell death; recovery; apoptosis; proliferation

1. Introduction

High-grade primary brain tumors such as glioblastoma (GBM) and secondary brain metastases (BM) remain a clinical challenge to treat despite years of dedicated research. Gliomas comprise approximately 80% of all primary malignant brain tumor diagnoses, with 6 in 100,000 people diagnosed annually in the United States [1]. Despite decades of research efforts, GBM prognosis remains grim with 5-year survival hovering at approximately 5% [1]. The current standard of care for high grade gliomas is a combination of maximum safe surgical resection, temozolomide chemotherapy, and radiotherapy [2, 3]. Surgical resection nearly doubles life expectancy and relieves patients of some tumor-associated symptoms. However, it is estimated that >98% extent of tumor resection is necessary to significantly improve survival, and GBM recurrence is still rarely prevented [4]. The aggressive nature of high-grade glioma cells [5], their resistance to chemotherapy and radiotherapy [6], minimal efficacy of chemotherapeutics due to ineffective delivery across the blood-brain barrier (BBB) [7, 8], and residual cell populations left behind following surgical resection all contribute to the inherent recurrence of GBM [4, 5]. The incidence of brain metastasis (BM) is estimated to be ~2-10 times greater than primary brain tumors like GBM, with an estimated 20-50% of patients diagnosed with certain cancers expected to develop BM in their lifetime [9-15]. Along with breast, colon, and renal cell carcinomas and melanoma, one of the most common cancers to result in BM are lung carcinomas [13-17], which account for ~10-20% of all cases of BM [13, 15, 18]. Standard treatments for BM, including surgery, stereotactic radiosurgery, and whole-brain radiotherapy harbor similar limitations to primary brain tumor therapies, with survival times for BM patients after these treatments remaining on the order of months [19-21].

The poor prognosis associated with current GBM and BM treatment modalities has led to substantial interest in various non- and minimally invasive ablative technologies for the treatment of primary and metastatic brain tumors. To that end, electroporation, the application of pulsed electric fields to a cell population to elevate transmembrane potential and result in the formation of nanopores in the plasma membrane, has gained interest as a therapeutic [22-24]. Depending on treatment parameters, membrane nanopores may reseal over time (reversible electroporation) or may result in irreparable damage, leading to cell death by irreversible electroporation (IRE). IRE has been applied clinically as a minimally-invasive, nonthermal ablative therapeutic for precise, targeted ablation of a variety of tissue and tumor types [25-30]. IRE pulses are typically high voltage, relatively long duration (100 μs) and unipolar, which can trigger muscle contractions, necessitating the use of neuromuscular blockade and cardiac synchronization during treatment [31-33]. These limitations are addressed by the development of high-frequency irreversible electroporation (H-FIRE), which utilizes high-frequency bipolar pulses to induce irreversible electroporation and death of treated cells while mitigating muscle contractions [30, 34].

H-FIRE has been shown to precisely and nonthermally ablate meningiomas in dogs diagnosed with the disease while sparing surrounding healthy brain tissue, demonstrating the applicability of H-FIRE as an alternative to surgical debulking of brain tumors [35]. Another potential clinical advantage of H-FIRE ablation is its entirely nonthermal mechanism of cell death, which is crucial for avoiding unwanted skull heating during treatment [30]. Additionally, both IRE and H-FIRE have been demonstrated to safely ablate primary brain tumors *in vivo* while simultaneously increasing peritumoral BBB permeability surrounding the zone of nonthermal ablation, which can be exploited for improved delivery of therapeutics to target infiltrative tumor cells [26, 35-38]. Further, the propensity of IRE and H-FIRE to stimulate both local and systemic immune responses has been described [25, 39-50]. However, the exact mechanisms of cell death that give rise to these observed downstream effects are not yet fully characterized. Preliminary investigations suggest that apoptosis, pyroptosis, and necrosis are likely involved [36, 46, 51], but little is known about potential mechanisms of cellular recovery which could lead to therapeutic resistance or tumor recurrence. Further, because treatment parameter optimization for H-FIRE treatments is highly complex, a complete understanding of H-FIRE-induced tumor cell death and recovery is critical for ensuring truly irreversible cell damage after treatment and prevention of tumor recurrence [52]. The intricacies of such treatment-induced cell death mechanisms weigh heavily on downstream changes in the local and systemic microenvironments, such as the engagement of the immune system and disruption of peritumoral BBB. Thus, additional work investigating the complexities of H-FIRE-induced tumor cell death and recovery mechanisms is urgently needed.

In this work, we modeled H-FIRE treatment of primary and metastatic brain tumors using rat glioma and murine Lewis lung carcinoma cell lines, respectively. The aim of this study was to characterize the *in vitro* dose-dependence and temporal profiles of cell membrane permeability, apoptosis, metabolic viability, and proliferative capacity of tumor cells treated with H-FIRE, to contribute to the characterization of H-FIRE-induced tumor cell death and recovery.

2. Materials and Methods

2.1 Cell culture

Murine Lewis lung carcinoma cell line LL/2 (LLC1) (ATCC, CRL-1642) and rat glioma cell line F98 (ATCC, CRL-2397) were grown in DMEM (ATCC, 30-2002) supplemented with 10% fetal bovine serum (Thermo Fisher Scientific, Gibco) and 1% penicillin-streptomycin (Thermo Fisher Scientific, Gibco). Cells were incubated at 37 °C in a humidified environment containing 5% CO_2 and subcultured regularly. All cells used were between passages 5 and 14, and were detached for use in experiments using TrypLE Express Enzyme at room temperature (Thermo Fisher Scientific, Gibco).

2.2 Cancer Cell H-FIRE treatment

At near confluence and following detachment with TrypLE, LL/2 and F98 cells were washed and resuspended in a 5.5:1 ratio of low-conductivity sucrose solution (85 g sucrose, 3 g glucose, 7.25 ml DMEM, and 992.75 ml DI water) to unsupplemented DMEM to a

concentration of 1.25×10^6 cells/ml. 800 μl of cell suspension were aliquoted into 4 mm sterile electroporation cuvettes (USA Scientific). H-FIRE pulse parameters were delivered to cuvettes using a custom-built H-FIRE pulse generator (VoltMed Inc, Blacksburg, VA). In order to maximize electroporation without inducing thermal cell death, preliminary experiments were carried out to determine the maximum electric field and number of bursts that could be delivered without raising temperature by more than 20°C during treatment. Temperature changes were measured by inserting a fiber optic temperature probe into the cuvette during treatment. It was determined that 200 bursts at an electric field strength of 3,000 V/cm was the maximum parameter combination to prevent significant temperature changes capable of inducing thermal cell death. Therefore, H-FIRE treatments consisted of 200 bursts of bipolar pulses delivered at a frequency of 1 burst per second, with electric fields escalating to 3,000 V/cm. An individual burst of bipolar pulses consisted of a 2 μs positive pulse, a 5 μs interphase delay, a 2 μs negative pulse, and a 5 μs interpulse delay (2-5-2 pattern) which was repeated until a total energized time of 100 μs was achieved. Treatment voltage and current were monitored using an oscilloscope. H-FIRE treatments consisting of these parameters were delivered at electric field magnitudes of 0, 750, 1,500, 2,500, and 3,000 V/cm. All H-FIRE treatments were performed in triplicates.

2.3 YO-PRO®-1/*PI*/*Hoechst-33342 assay*

Immediately following treatment, cells were removed from electroporation cuvettes and centrifuged at 250 x g for 6 minutes. Triplicate aliquots of 100,000 cells were removed for staining for the immediate post-treatment time point, and remaining cells were divided equally in 12-well plates for analysis 6h and 24h post-treatment in triplicates. Membrane permeability and apoptosis were measured using Chromatin Condensation and Membrane Permeability Dead Cell Apoptosis Kit with Hoechst 33342, YO-PRO®-1, and propidium iodide (PI) dyes (Thermo Fisher) following manufacturers protocol. Cells were analyzed by flow cytometry in duplicates (Cytoflex, Beckman Coulter). In addition to the sham (0 V/cm) treatment group, the electric field for each cell line that did not result in significant recovery of membrane integrity by 24h was deemed “recovery-inhibiting” and carried forward for subsequent assays. The lowest electric field for each cell line that did result in significant recovery of membrane integrity by 24h was deemed “recovery-permitting” and also carried forward for subsequent assays.

2.4 WST-8 metabolic viability assay

Immediately following treatment, cell suspensions were diluted with complete electroporation buffer, and 10,000 cells were plated in a 96-well plate in triplicates to be analyzed immediately post-treatment. Remaining cells were centrifuged at 250 x g for 6 minutes, resuspended in complete media, and plated and incubated at a density of 1×10^5 cells/ml in triplicates in 96-well plates to be analyzed 6h and 24h post-treatment. At indicated time points, cells were lysed and evaluated for metabolic viability using the WST-8 Cytotoxicity Assay (abcam) per manufacturers protocol.

2.5 Clonogenic proliferation assay

After H-FIRE treatment, cell suspensions were centrifuged at 250 x g for 6 minutes and resuspended in complete media. Cells were plated in 10 mm cell culture dishes (Millipore

Sigma) at appropriate densities. LL/2 cells treated at 0, 1,500, and 3,000 V/cm were plated at densities of 100, 500, and 1,000 cells/dish respectively, and incubated for 7 days. F98 cells treated at 0, 1,500, and 3,000 V/cm were plated at densities of 500, 1,000, and 10,000 cells/dish respectively, and incubated for 8 days. Media was refreshed 24h after plating. After the indicated incubation period, cells were washed twice with ice-cold PBS. Cells were fixed with 100% ice-cold methanol for 12 minutes, and rinsed twice again with ice-cold PBS. Cells were stained with 0.5% w/v crystal violet in DI water for 45 minutes. Dishes were rinsed in tap water, and colonies were counted and photographed using an inverted microscope (Olympus IX37). Colonies were defined as containing ≥50 cells each. Plating efficiency of sham-treated cells (Equation 1) and survival fractions of treated cells (Equation 2) were calculated.

$$\text{Plating efficiency (PE)}_{\text{sham}} = \frac{(\text{no. colonies formed})_{\text{sham}}}{(\text{no. cells seeded})_{\text{sham}}} \quad (1)$$

$$\text{Survival fraction (SE)}_{\text{treated}} = \frac{(\text{no. colonies formed})_{\text{treated}}}{(\text{no. cells seeded})_{\text{treated}} \times (\text{PE})_{\text{sham}}} \quad (2)$$

2.6 Statistical analysis

All experiments were performed with at least three replicates per experiment. Results are presented as mean ± standard deviation (SD) unless otherwise noted. For evaluation of statistical significance of permeability, apoptosis, and metabolic viability data, two-way ANOVA with multiple comparisons and Tukey post-hoc test was used. For evaluation of statistical significance of proliferation, ordinary one-way ANOVA with multiple comparisons and Tukey post-hoc test was used. Statistical analysis was performed on Graphpad Prism 9 for Mac OS, (GraphPad Software, San Diego, California USA, www.graphpad.com).

3. Results

3.1. Dose-dependent irreversible and recoverable permeabilization

Preliminary experiments quantifying treatment-induced temperature changes demonstrated that the maximum parameter combination to prevent temperature changes capable of inducing thermal cell death was 200 bursts of 3,000 V/cm electric field (data not shown). All subsequent treatments consisted of 200 bursts of electric field magnitudes less than or equal to 3,000 V/cm. Membrane permeability to YO-PRO®-1 and PI was assessed at specific time points post-treatment for tumor cell lines treated with escalating H-FIRE electric fields according to these parameters. The percentage of tumor cells permeable to YO-PRO®-1 and PI increased as H-FIRE electric fields escalated (Fig. 1a, 1b). Statistically significant differences in immediate post-treatment permeability ($p<0.05$) compared to sham were observed at electric fields of 1,500 V/cm and above for LL/2 cells, and 750 V/cm and above for F98 cells (Fig 1b). For LL/2 cells, all electric fields 1,500 V/cm and above induced permeability changes that were significantly different from the immediately preceding

electric field (Fig 1b). For F98 cells, only 1,500 V/cm induced permeability changes that were significantly different from the immediately preceding electric field (Fig 1b).

For both tumor cell lines, electric fields were identified that induced permeabilization that did and did not significantly ($p<0.05$) recover by 24 hours post-treatment. When compared to the immediate post-treatment timepoint, electric fields of 1,500 V/cm induced permeability changes that recovered significantly by the 24 hour timepoint for both cell lines (Fig. 1c). Likewise, electric fields of 3,000 V/cm induced permeability changes that did not significantly recover by 24 hours for both cell lines (Fig 1c). Initial permeability of sham-treated F98 cells significantly recovered by 24 hours post treatment. The LL/2 cells did not exhibit statistically significant differences in permeability by 24 hours post treatment. F98 cells treated with 3,000 V/cm exhibited significantly increased permeability at 24 hours compared to immediate post-treatment, while no such differences were found in LL/2 cells.

3.2 Dose-dependent irreversible and recoverable apoptosis and metabolic viability

Chromatin condensation is a well-established step of apoptosis [53], and Hoechst-33342 is a DNA-binding dye that dimly stains chromatin of viable cells while brightly staining condensed chromatin, an identifying characteristic of apoptotic cells. We assessed chromatin condensation at specific time points post-treatment for tumor cell lines treated with escalating H-FIRE electric fields to quantify apoptosis. The percentage of tumor cells that stained brightly with Hoechst-33342 increased with escalating H-FIRE electric fields (Fig. 2a, 2b). Statistically significant increases in immediate post-treatment chromatin condensation ($p<0.05$) compared to sham were observed at electric fields of 1,500 V/cm and above for LL/2 and F98 cells (Fig 2b). For LL/2 cells, all electric fields 1,500 V/cm and above induced significantly increased chromatin condensation compared to the immediately preceding electric field (Fig 2b). For F98 cells, only 1,500 V/cm induced significantly more chromatin condensation compared to the immediately preceding electric field (Fig 2b).

In order to further investigate potential recovery of cellular damage induced by H-FIRE, we identified electric fields for both tumor cell lines that induced permeabilization that did and did not significantly ($p<0.05$) recover by 24 hours post-treatment (Fig 1c). These electric fields were 1,500 and 3,000 V/cm, respectively. For both tumor cell lines, Hoechst-33342 staining of condensed chromatin exhibited statistically significant recovery by 24 hours post-treatment at 1,500 V/cm (Fig 2c). Likewise, there was no statistically significant recovery of chromatin condensation by 24 hours post-treatment in the 3,000 V/cm group. Initial chromatin condensation of sham-treated F98 cells significantly recovered by 24 hours post treatment, while sham-treated LL/2 cells did not exhibit statistically significant differences in chromatin condensation by 24 hours post treatment. LL/2 cells treated with 3,000 V/cm exhibited significantly increased chromatin condensation at 24 hours compared to immediate post-treatment, while no such differences were found in F98 cells (Fig 2c).

WST-8 was used to quantify mitochondrial/metabolic viability of tumor cell lines at selected timepoints after treatment with recovery-permitting and -inhibiting H-FIRE electric fields (1,500 and 3,000 V/cm, respectively). NADH produced in the mitochondria reduces WST-8 tetrazolium salt, producing a fluorescent dye indicating metabolically active cells. LL/2

cells treated with 1,500 and 3,000 V/cm had significantly decreased WST-8 fluorescence relative to sham at the immediate timepoint (Fig 2d). No statistically significant differences in WST-8 fluorescence relative to sham were noted for F98 cells at the immediate timepoint treated with 1,500 or 3,000 V/cm, but nonstatistically significant dose-dependent trends were noted. No statistically significant differences relative to sham were noted for LL/2 or F98 cells at the immediate or 6 hour timepoints (Fig 2d). At the 24 hour timepoint, LL/2 and F98 cells treated with 3,000 V/cm had significantly reduced WST-8 fluorescence relative to sham. F98 cells treated with 1,500 V/cm also had significantly reduced WST-8 fluorescence relative to sham at 24 hours. Compared to the immediate post-treatment timepoint, no significant differences in relative WST-8 fluorescence were noted for LL/2 or F98 cells treated with 1,500 V/cm by 24 hours post treatment, but nonstatistically significant time-dependent trends were noted for both cell lines. Compared to the immediate post-treatment timepoint, significant decreases in relative WST-8 fluorescence were noted for LL/2 cells treated with 3,000 V/cm by 24 hours post treatment, while nonstatistically significant time-dependent decreases were noted for F98 cells treated at the same electric field (Fig 2d).

3.3 Tumor cell proliferative capacity is consistent with recovery of H-FIRE-induced damage

Clonogenic assays were used to assess proliferative capacity of tumor cell lines treated with H-FIRE at selected field strengths observed to permit and inhibit significant recovery of membrane permeability (1,500 V/cm and 3,000 V/cm, respectively) (Fig. 3b). Both LL/2 and F98 cells treated with 1,500 V/cm had significantly decreased survival fractions relative to sham (0.134 and 0.449, respectively) (Fig. 3a). Both LL/2 and F98 cells treated with 3,000 V/cm had significantly reduced survival fractions relative to sham (0.009 and 0.014, respectively), but only LL/2 cells treated at this electric field had statistically significant reduced survival fraction relative to 1,500 V/cm (Fig. 3a).

4. Discussion

Our results indicate that H-FIRE induces cellular damage in a dose-dependent manner in our model cell lines. This damage includes cell membrane permeabilization, apoptosis, and interference with mitochondrial metabolic activity. Our data also show specific H-FIRE electric field doses induce cell membrane permeabilization that recovers significantly by 24 hours post-treatment, supporting our hypothesis that tumor cells treated with specific H-FIRE electric field doses can repair induced cellular damage. Results of clonogenic assays suggest that cancer cell lines treated with H-FIRE electric field doses that permitted recovery of cellular damage maintain their proliferative capacity, while those treated with doses that inhibited recovery are unable to proliferate.

We measured permeability of H-FIRE treated cancer cells to exclusion dyes YO-PRO®-1 and PI at selected timepoints post-treatment to quantify induced cell membrane permeabilization and recovery of membrane integrity. We demonstrate electric field dose-dependent permeabilization of these cancer cell lines immediately post-treatment, in agreement with previous studies of H-FIRE [46, 51]. We show that specific H-FIRE electric field doses allow statistically significant recovery of membrane permeability to these

exclusion dyes. However, tumor cells treated with higher electric fields do not significantly recover membrane integrity by the same timepoint, suggesting the tentative presence of a cell membrane recovery activity at certain H-FIRE doses. This is in agreement with a previous study of H-FIRE permeabilization up to 3 hours post-treatment, that demonstrated significant recovery of YO-PRO®-1 permeability of pancreatic adenocarcinoma cells within one hour of treatment [51]. They similarly found that an electric field of 1,100 V/cm permitted this membrane recovery, while 3,800 V/cm did not. For both of our tumor cell lines, the observed recovery of cell membrane integrity occurred when cells were treated with 1,500 V/cm, while 3,000 V/cm treatments induced irreversible cell membrane damage with no recovery by 24 hours post-treatment. We noted similar escalation of cell membrane permeability to YO-PRO®-1 and PI for both F98 and LL/2 tumor cell lines, but F98 cells were more sensitive to the experimental setup required for treatment. Specifically, the sham-treated cells exhibited substantially higher YO-PRO®-1 and PI permeability at the immediate timepoint, but recovered significantly by the 24 hour timepoint. However, F98 cells treated at an electric field strength of 3,000 V/cm did not recover by the 24 hour timepoint, demonstrating distinct treatment-induced effects, and not just sensitivity to experimental setup. Although not within the scope of our study, future work should seek to identify and characterize specific mechanisms of cell membrane repair.

Consistent with previous studies of variable pulsed electric fields and irreversible electroporation, our study confirms apoptosis as a component of the mechanism of *in vitro* H-FIRE-induced cell death, as evidenced by treatment-induced chromatin condensation [46, 51, 54-59]. Other studies have additionally implicated necrosis and pyroptosis [46, 59] in electroporation-induced cell death. Further investigation of the involvement of multiple mechanisms in H-FIRE-specific cell death are warranted. In line with the dose-dependent trends of cell membrane permeabilization, both tumor cell lines exhibited increasing chromatin condensation when treated with escalating H-FIRE electric fields. Similarly, F98 cells exhibited chromatin condensation at lower electric fields where LL/2 cells did not, indicating potential cell-dependent treatment sensitivities. Chromatin condensation of sham-treated F98 cells also significantly recovered by the 24 hour timepoint. Following the same trends as cell membrane permeability, tumor cell lines treated with 1,500 V/cm (membrane recovery-permitting) also significantly recovered chromatin configuration by 24 hours, whereas those treated with 3,000 V/cm (membrane recovery-inhibiting) did not recover chromatin configuration in the same time. This suggests a relationship between irreversible membrane permeabilization and a lack of recovery from the apoptotic cascade. Likewise, the recovery of chromatin condensation by tumor cells treated with 1,500 V/cm suggests that irreversible membrane permeabilization is required to induce irreversible apoptosis. One *in vivo* study of IRE ablation of gastric tissue demonstrated recovery of apoptosis within the treated lesion 10 hours after ablation, which was presumed to be a result of robust metabolic activity from blood circulation [60]. Here, we have demonstrated such apoptotic recovery *in vitro* in the absence of blood-flow, suggesting the presence of an intracellular, blood flow-independent mechanism of apoptotic recovery.

To further characterize cellular damage, death, and recovery induced by H-FIRE, we temporally analyzed the reduction of WST-8 by tumor cells treated with sham, membrane recovery-permitting (1,500 V/cm), and membrane recovery-inhibiting (3,000 V/cm) doses of

H-FIRE. WST-8 is a tetrazolium salt that, upon reduction by the mitochondrial coenzyme NADH, produces a fluorescent dye which can be used to quantify the mitochondrial synthesis of NADH and thus indicate metabolic viability of cells. Our data show that, consistent with recovery or irreversibility of membrane permeability and apoptosis, tumor cells treated with 1,500 V/cm trended toward recovery of metabolic viability by 24 hours. Significant recovery of metabolic viability by F98 cells treated with 1,500 V/cm is apparent, although metabolic deficiency is more substantial in F98 cells than LL/2 cells treated with the same electric field. That is to say, F98 cells again appear to be more sensitive to H-FIRE treatment than LL/2 cells. Both tumor cell lines treated with 3,000 V/cm were significantly less metabolically active 24 hours post-treatment than immediately post-treatment, suggesting a progressive loss and obvious lack of recovery of metabolic activity when treated with H-FIRE doses that inhibit recovery of membrane integrity and apoptosis. These data further suggest that irreversible membrane permeabilization is required to irreversibly kill tumor cells, and that recovery of such membrane permeabilization may allow cells to recover other viability functions. Previous studies have similarly demonstrated the impact of other irreversible electroporation protocols on mitochondrial function [61-63]. To the best of our knowledge, our study is the first to demonstrate H-FIRE's direct impact on tumor cell mitochondrial function and dose-dependent metabolic recovery.

To test whether or not tumor cells that demonstrated recovery or irreversible damage could proliferate, we employed clonogenic assays. Although tumor cells treated with 1,500 V/cm had significantly reduced survival fractions relative to sham, they maintained some level of proliferative capacity, as evidenced by survival fractions of >0.1 for both cell lines treated with this dose. In other words, LL/2 and F98 cells treated with 1,500 V/cm proliferated with 13% and 45% of the proliferative capacity of the sham, respectively. Although significantly reduced relative to sham, these maintained proliferative capacities could present a significant threat of tumor recurrence *in vivo*. Glioma cells that are able to repair damage and survive radiation treatment are known to give rise to radioresistant populations and tumor recurrence [64]. It is estimated that >98% reduction of tumor volume is necessary to prevent recurrence and improve survival of GBM patients [4]. Due to similar pitfalls of resistance and tumor cell survival after therapy, BM recurrence occurs in approximately 10-34% of patients even after complete surgical resection and radiotherapy [65-67]. In our study, the survival fractions of tumor cells treated with recovery-inhibiting doses of H-FIRE did not exceed 0.01, and therefore are suggestive of a potentially reduced risk of tumor recurrence. Though these results suggest the dose-dependence of long-term tumor cell proliferation, these findings must be further confirmed *in vivo* to identify potentially dose-dependent tumor recurrence.

Although we demonstrate the relationship between dose-dependent recoverable and irreversible cellular damage and proliferative capacity of cancer cells treated with H-FIRE, our study is subject to typical limitations of *in vitro* electroporation. Specifically, the use of a cancer cell suspension model alters the morphology of cancer cells relative to *in vivo*. This altered morphology increases electric field thresholds for electroporation [68], and therefore the specific electric field thresholds required to induce the described effects *in vivo* must first be determined for cells with physiologically-representative morphology. It has also been shown that the presence of calcium during electroporation treatments can

alter the dynamics of electroporation. Specifically, Ciobanu et al. demonstrated that cells electroporated in the presence of calcium ($[Ca^{2+}]<0.5$ mM) were less permeable to PI than cells electroporated in the absence of calcium five minutes post-treatment, suggesting that low calcium concentrations may contribute to the resealing of membrane pores at early timepoints [69, 70]. The complete electroporation buffer used in the present study contains approximately 0.3 mM calcium, which may contribute to the dose-dependent membrane recovery effects demonstrated and the relatively high H-FIRE electric field doses required to induce damage without recovery. Further, due to temperature concerns and the goal of maximum electroporation, cancer cells were suspended in a low-conductivity sucrose-based buffer solution instead of media. F98 cells proved sensitive to this buffer solution as demonstrated by elevated permeability in the sham group immediately post-treatment. Although significant recovery of membrane function occurred by 24 hours post-treatment, this sensitivity must be noted when interpreting potential cell-specific dose effects. Finally, although we demonstrate consistent trends between cellular damage recovery and proliferative capacity, causative relationships between individual metrics of cellular damage, as we have described them, and proliferative capacity cannot be inferred from the present study.

5. Conclusions

We demonstrated that H-FIRE exerts electric field-dependent cell membrane permeabilization. We also showed that tumor cells treated with certain H-FIRE doses tentatively possess recovery mechanisms that allow for repair of induced membrane damage, apoptosis, and metabolic dysfunction. These recovery mechanisms may ultimately allow tumor cells to survive and proliferate following permitting doses of H-FIRE. The results of our study highlight the importance of choosing appropriate pulsing parameters, potentially specific to tumor cell type. Our study suggests that H-FIRE pulsing protocols intended to induce irreversible cell death may still permit recovery of cellular damage and eventually proliferation of tumor cells. At the same time, we have shown that higher doses of H-FIRE effectively suppress cellular damage recovery and tumor cell proliferation *in vitro*, supporting the therapeutic potential of H-FIRE to control highly-recurrent primary and metastatic brain tumors.

Acknowledgements

We would like to acknowledge the contributions of Joanne Tuohy, Shawna Klahn, Jennifer Carroll, and Melvin Lorenzo in their contributions to data discussion and preparation of this manuscript.

Funding

This work was supported by the National Institutes of Health [R01CA213423)] and the Grayton Friedlander Memorial Fund.

References

[1]. Ostrom QT, Gittleman H, Fulop J, Liu M, Blanda R, Kromer C, Wolinsky Y, Kruchko C, Barnholtz-Sloan JS, CBTRUS Statistical Report: Primary Brain and Central Nervous System Tumors Diagnosed in the United States in 2008-2012, Neuro Oncol, 17 Suppl 4 (2015) iv1–iv62. [PubMed: 26511214]

[2]. Stupp R, Mason WP, van den Bent MJ, Weller M, Fisher B, Taphoorn MJ, Belanger K, Brandes AA, Marosi C, Bogdahn U, Curschmann J, Janzer RC, Ludwin SK, Gorlia T, Allgeier A, Lacombe D, Cairncross JG, Eisenhauer E, Mirimanoff RO, R. European Organisation for, T. Treatment of Cancer Brain, G. Radiotherapy, G. National Cancer Institute of Canada Clinical Trials, Radiotherapy plus concomitant and adjuvant temozolomide for glioblastoma, N Engl J Med, 352 (2005) 987–996. [PubMed: 15758009]

[3]. Stupp R, Hegi ME, Mason WP, van den Bent MJ, Taphoorn MJ, Janzer RC, Ludwin SK, Allgeier A, Fisher B, Belanger K, Hau P, Brandes AA, Gijtenbeek J, Marosi C, Vecht CJ, Mokhtari K, Wesseling P, Villa S, Eisenhauer E, Gorlia T, Weller M, Lacombe D, Cairncross JG, Mirimanoff RO, R. European Organisation for, T. Treatment of Cancer Brain, G. Radiation Oncology, G. National Cancer Institute of Canada Clinical Trials, Effects of radiotherapy with concomitant and adjuvant temozolomide versus radiotherapy alone on survival in glioblastoma in a randomised phase III study: 5-year analysis of the EORTC-NCIC trial, Lancet Oncol, 10 (2009) 459–466. [PubMed: 19269895]

[4]. Lacroix M, Abi-Said D, Fourney DR, Gokaslan ZL, Shi W, DeMonte F, Lang FF, McCutcheon IE, Hassenbusch SJ, Holland E, Hess K, Michael C, Miller D, Sawaya R, A multivariate analysis of 416 patients with glioblastoma multiforme: prognosis, extent of resection, and survival, J Neurosurg, 95 (2001) 190–198.

[5]. la Fougere C, Suchorska B, Bartenstein P, Kreth FW, Tonn JC, Molecular imaging of gliomas with PET: opportunities and limitations, Neuro Oncol, 13 (2011) 806–819. [PubMed: 21757446]

[6]. Hegi ME, Diserens AC, Gorlia T, Hamou MF, de Tribolet N, Weller M, Kros JM, Hainfellner JA, Mason W, Mariani L, Bromberg JE, Hau P, Mirimanoff RO, Cairncross JG, Janzer RC, Stupp R, MGMT gene silencing and benefit from temozolomide in glioblastoma, N Engl J Med, 352 (2005) 997–1003. [PubMed: 15758010]

[7]. Elmeliegy MA, Carcaboso AM, Tagen M, Bai F, Stewart CF, Role of ATP-binding cassette and solute carrier transporters in erlotinib CNS penetration and intracellular accumulation, Clin Cancer Res, 17 (2011) 89–99. [PubMed: 21088257]

[8]. Agarwal S, Sane R, Gallardo JL, Ohlfest JR, Elmquist WF, Distribution of gefitinib to the brain is limited by P-glycoprotein (ABCB1) and breast cancer resistance protein (ABCG2)-mediated active efflux, J Pharmacol Exp Ther, 334 (2010) 147–155. [PubMed: 20421331]

[9]. Gavrilovic IT, Posner JB, Brain metastases: epidemiology and pathophysiology, J Neurooncol, 75 (2005) 5–14. [PubMed: 16215811]

[10]. Davis FG, Dolecek TA, McCarthy BJ, Villano JL, Toward determining the lifetime occurrence of metastatic brain tumors estimated from 2007 United States cancer incidence data, Neuro Oncol, 14 (2012) 1171–1177. [PubMed: 22898372]

[11]. Nathoo N, Chahlavi A, Barnett GH, Toms SA, Pathobiology of brain metastases, J Clin Pathol, 58 (2005) 237–242. [PubMed: 15735152]

[12]. DiStefano A, Yap Y. Yong, Hortobagyi GN, Blumenschein GR, The natural history of breast cancer patients with brain metastases, Cancer, 44 (1979) 1913–1918. [PubMed: 498057]

[13]. Barnholtz-Sloan JS, Sloan AE, Davis FG, Vigneau FD, Lai P, Sawaya RE, Incidence proportions of brain metastases in patients diagnosed (1973 to 2001) in the Metropolitan Detroit Cancer Surveillance System, J Clin Oncol, 22 (2004) 2865–2872. [PubMed: 15254054]

[14]. Patel JK, Didolkar MS, Pickren JW, Moore RH, Metastatic pattern of malignant melanoma. A study of 216 autopsy cases, Am J Surg, 135 (1978) 807–810. [PubMed: 665907]

[15]. Schouten LJ, Rutten J, Huveneers HA, Twijnstra A, Incidence of brain metastases in a cohort of patients with carcinoma of the breast, colon, kidney, and lung and melanoma, Cancer, 94 (2002) 2698–2705. [PubMed: 12173339]

[16]. MacDonald NJ, Steeg PS, Molecular basis of tumour metastasis, Cancer Surv, 16 (1993) 175–199. [PubMed: 7688661]

[17]. Chambers AF, MacDonald IC, Schmidt EE, Morris VL, Groom AC, Clinical targets for anti-metastasis therapy, Adv Cancer Res, 79 (2000) 91–121. [PubMed: 10818678]

[18]. Waqar SN, Samson PP, Robinson CG, Bradley J, Devarakonda S, Du L, Govindan R, Gao F, Puri V, Morgensztern D, Non-small-cell Lung Cancer With Brain Metastasis at Presentation, Clin Lung Cancer, 19 (2018) e373–e379. [PubMed: 29526531]

[19]. van den Bent MJ, The diagnosis and management of brain metastases, Curr Opin Neurol, 14 (2001) 717–723. [PubMed: 11723379]

[20]. Mehta MP, Rodrigus P, Terhaard CH, Rao A, Suh J, Roa W, Souhami L, Bezjak A, Leibenhaut M, Komaki R, Schultz C, Timmerman R, Curran W, Smith J, Phan SC, Miller RA, Renschler MF, Survival and neurologic outcomes in a randomized trial of motexafin gadolinium and whole-brain radiation therapy in brain metastases, J Clin Oncol, 21 (2003) 2529–2536. [PubMed: 12829672]

[21]. Hall WA, Djalilian HR, Nussbaum ES, Cho KH, Long-term survival with metastatic cancer to the brain, Med Oncol, 17 (2000) 279–286. [PubMed: 11114706]

[22]. Kotnik T, Pucihar G, Miklavcic D, Induced transmembrane voltage and its correlation with electroporation-mediated molecular transport, J Membr Biol, 236 (2010) 3–13. [PubMed: 20617432]

[23]. Ivey JW, Latouche EL, Sano MB, Rossmeisl JH, Davalos RV, Verbridge SS, Targeted cellular ablation based on the morphology of malignant cells, Sci Rep, 5 (2015) 17157. [PubMed: 26596248]

[24]. Davalos RV, Mir IL, Rubinsky B, Tissue ablation with irreversible electroporation, Ann Biomed Eng, 51 (2005) 5617–5622.

[25]. Partridge BR, O'Brien TJ, Lorenzo MF, Coutermarsh-Ott SL, Barry SL, Stadler K, Muro N, Meyerhoeffer M, Allen IC, Davalos RV, Dervisis NG, High-Frequency Irreversible Electroporation for Treatment of Primary Liver Cancer: A Proof-of-Principle Study in Canine Hepatocellular Carcinoma, J Vasc Interv Radiol, 31 (2020) 482–491 e484. [PubMed: 31956003]

[26]. Rossmeisl JH Jr., Garcia PA, Pancotto TE, Robertson JL, Henao-Guerrero N, Neal RE 2nd, Ellis TL, Davalos RV, Safety and feasibility of the NanoKnife system for irreversible electroporation ablative treatment of canine spontaneous intracranial gliomas, J Neurosurg, 123 (2015) 1008–1025. [PubMed: 26140483]

[27]. van Es R, Konings MK, Du Pre BC, Neven K, van Wessel H, van Driel V, Westra AH, Doevendans PAF, Wittkampf FHM, High-frequency irreversible electroporation for cardiac ablation using an asymmetrical waveform, Biomed Eng Online, 18 (2019) 75. [PubMed: 31221146]

[28]. Dong S, Wang H, Zhao Y, Sun Y, Yao C, First Human Trial of High-Frequency Irreversible Electroporation Therapy for Prostate Cancer, Technol Cancer Res Treat, 17 (2018) 1533033818789692. [PubMed: 30045668]

[29]. Rolong A, Schmelz EM, Davalos RV, High-frequency irreversible electroporation targets resilient tumor-initiating cells in ovarian cancer, Integr Biol (Camb), 9 (2017) 979–987. [PubMed: 29186222]

[30]. Arena CB, Sano MB, Rossmeisl JH Jr., Caldwell JL, Garcia PA, Rylander MN, Davalos RV, High-frequency irreversible electroporation (H-FIRE) for non-thermal ablation without muscle contraction, Biomed Eng Online, 10 (2011) 102. [PubMed: 22104372]

[31]. Ball C, Thomson KR, Kavnoudias H, Irreversible electroporation: a new challenge in "out of operating theater" anesthesia, Anesth Analg, 110 (2010) 1305–1309. [PubMed: 20142349]

[32]. Rubinsky B, Onik G, Mikus P, Irreversible electroporation: a new ablation modality--clinical implications, Technol Cancer Res Treat, 6 (2007) 37–48. [PubMed: 17241099]

[33]. Landstrom FJ, Nilsson CO, Crafoord S, Reizenstein JA, Adamsson GB, Lofgren LA, Electroporation therapy of skin cancer in the head and neck area, Dermatol Surg, 36 (2010) 1245–1250. [PubMed: 20666812]

[34]. Bhonsle SP, Arena CB, Sweeney DC, Davalos RV, Mitigation of impedance changes due to electroporation therapy using bursts of high-frequency bipolar pulses, Biomed Eng Online, 14 Suppl 3 (2015) S3.

[35]. Latouche EL, Arena CB, Ivey JW, Garcia PA, Pancotto TE, Pavlisko N, Verbridge SS, Davalos RV, Rossmeisl JH, High-Frequency Irreversible Electroporation for Intracranial Meningioma: A Feasibility Study in a Spontaneous Canine Tumor Model, Technol Cancer Res Treat, 17 (2018) 1533033818785285. [PubMed: 30071778]

[36]. Rossmeisl JH Jr., Garcia PA, Roberston JL, Ellis TL, Davalos RV, Pathology of non-thermal irreversible electroporation (N-TIRE)-induced ablation of the canine brain, J Vet Sci, 14 (2013) 433–440. [PubMed: 23820168]

[37]. Garcia PA, Pancotto T, Rossmeisl JH Jr., Henao-Guerrero N, Gustafson NR, Daniel GB, Robertson JL, Ellis TL, Davalos RV, Non-thermal irreversible electroporation (N-TIRE) and adjuvant fractionated radiotherapeutic multimodal therapy for intracranial malignant glioma in a canine patient, Technol Cancer Res Treat, 10 (2011) 73–83. [PubMed: 21214290]

[38]. Sharabi S, Kos B, Last D, Guez D, Daniels D, Harnof S, Mardor Y, Miklavcic D, A statistical model describing combined irreversible electroporation and electroporation-induced blood-brain barrier disruption, Radiol Oncol, 50 (2016) 28–38. [PubMed: 27069447]

[39]. Chen X, Ren Z, Yin S, Xu Y, Guo D, Xie H, Zhou L, Wu L, Jiang J, Li H, Sun J, Zheng S, The local liver ablation with pulsed electric field stimulate systemic immune reaction against hepatocellular carcinoma (HCC) with time-dependent cytokine profile, Cytokine, 93 (2017) 44–50. [PubMed: 28506570]

[40]. Al-Sakere B, Bernat C, Andre F, Connault E, Opolon P, Davalos RV, Mir LM, A study of the immunological response to tumor ablation with irreversible electroporation, Technol Cancer Res Treat, 6 (2007) 301–306. [PubMed: 17668937]

[41]. He C, Huang X, Zhang Y, Lin X, Li S, T-cell activation and immune memory enhancement induced by irreversible electroporation in pancreatic cancer, Clin Transl Med, (2020).

[42]. Li X, Xu K, Li W, Qiu X, Ma B, Fan Q, Li Z, Immunologic response to tumor ablation with irreversible electroporation, PLoS One, 7 (2012) e48749. [PubMed: 23139816]

[43]. Neal RE 2nd, Rossmeisl JH Jr., Robertson JL, Arena CB, Davis EM, Singh RN, Stallings J, Davalos RV, Improved local and systemic anti-tumor efficacy for irreversible electroporation in immunocompetent versus immunodeficient mice, PLoS One, 8 (2013) e64559. [PubMed: 23717630]

[44]. Pandit H, Hong YK, Li Y, Rostas J, Pulliam Z, Li SP, Martin RCG, Evaluating the Regulatory Immunomodulation Effect of Irreversible Electroporation (IRE) in Pancreatic Adenocarcinoma, Ann Surg Oncol, 26 (2019) 800–806.

[45]. Polajzer T, Jarm T, Miklavcic D, Analysis of damage-associated molecular pattern molecules due to electroporation of cells in vitro, Radiol Oncol, 54 (2020) 317–328. [PubMed: 32726295]

[46]. Ringel-Scaia VM, Beitel-White N, Lorenzo MF, Brock RM, Huie KE, Coutermarsh-Ott S, Eden K, McDaniel DK, Verbridge SS, Rossmeisl JH Jr., Oestreich KJ, Davalos RV, Allen IC, High-frequency irreversible electroporation is an effective tumor ablation strategy that induces immunologic cell death and promotes systemic anti-tumor immunity, EBioMedicine, 44 (2019) 112–125. [PubMed: 31130474]

[47]. Scheffer HJ, Stam AGM, Geboers B, Vroomen L, Ruarus A, de Bruijn B, van den Tol MP, Kazemier G, Meijerink MR, de Gruijl TD, Irreversible electroporation of locally advanced pancreatic cancer transiently alleviates immune suppression and creates a window for antitumor T cell activation, Oncoimmunology, 8 (2019) 1652532. [PubMed: 31646081]

[48]. Sugimoto K, Kakimi K, Takeuchi H, Fujieda N, Saito K, Sato E, Sakamaki K, Moriyasu F, Itoi T, Irreversible Electroporation versus Radiofrequency Ablation: Comparison of Systemic Immune Responses in Patients with Hepatocellular Carcinoma, J Vasc Interv Radiol, 30 (2019) 845–853 e846. [PubMed: 31126596]

[49]. White SB, Zhang Z, Chen J, Gogineni VR, Larson AC, Early Immunologic Response of Irreversible Electroporation versus Cryoablation in a Rodent Model of Pancreatic Cancer, J Vasc Interv Radiol, 29 (2018) 1764–1769. [PubMed: 30316676]

[50]. Zhao J, Wen X, Tian L, Li T, Xu C, Wen X, Melancon MP, Gupta S, Shen B, Peng W, Li C, Irreversible electroporation reverses resistance to immune checkpoint blockade in pancreatic cancer, Nat Commun, 10 (2019) 899. [PubMed: 30796212]

[51]. Mercadal B, Beitel-White N, Aycock KN, Castellvi Q, Davalos RV, Ivorra A, Dynamics of Cell Death After Conventional IRE and H-FIRE Treatments, Ann Biomed Eng, 48 (2020) 1451–1462. [PubMed: 32026232]

[52]. Zappatore M, Cerfeda G, Merla C, Tarricone L, Machine Learning for H-FIRE Protocols: Tuning Parameters for High-Frequency Irreversible Electroporation by Machine Learning, IEEE Microwave Magazine, 22 (2021) 42–59.

[53]. Wyllie AH, Beattie GJ, Hargreaves AD, Chromatin changes in apoptosis, Histochem J, 13 (1981) 681–692. [PubMed: 6975767]

[54]. Lopez-Alonso B, Hernaez A, Sarnago H, Naval A, Guemes A, Junquera C, Burdio JM, Castiella T, Monleon E, Gracia-Llanes J, Burdio F, Mejia E, Lucia O, Histopathological and Ultrastructural Changes after Electroporation in Pig Liver Using Parallel-Plate Electrodes and High-Performance Generator, Sci Rep, 9 (2019) 2647. [PubMed: 30804395]

[55]. Beebe SJ, Fox PM, Rec LJ, Willis EL, Schoenbach KH, Nanosecond, high-intensity pulsed electric fields induce apoptosis in human cells, FASEB J, 17 (2003) 1493–1495. [PubMed: 12824299]

[56]. Hofmann F, Ohnimus H, Scheller C, Strupp W, Zimmermann U, Jassoy C, Electric field pulses can induce apoptosis, J Membr Biol, 169 (1999) 103–109. [PubMed: 10341032]

[57]. Lee EW, Chen C, Prieto VE, Dry SM, Loh CT, Kee ST, Advanced hepatic ablation technique for creating complete cell death: irreversible electroporation, Radiology, 255 (2010) 426–433. [PubMed: 20413755]

[58]. Zhang Y, Lyu C, Liu Y, Lv Y, Chang TT, Rubinsky B, Molecular and histological study on the effects of non-thermal irreversible electroporation on the liver, Biochem Biophys Res Commun, 500 (2018) 665–670. [PubMed: 29678581]

[59]. Pinero J, Lopez-Baena M, Ortiz T, Cortes F, Apoptotic and necrotic cell death are both induced by electroporation in HL60 human promyeloid leukaemia cells, Apoptosis, 2 (1997) 330–336. [PubMed: 14646546]

[60]. Lee JM, Choi HS, Kim ES, Keum B, Seo YS, Jeen YT, Lee HS, Chun HJ, Um SH, Kim CD, Kim HB, Characterization of irreversible electroporation on the stomach: A feasibility study in rats, Sci Rep, 9 (2019) 9094. [PubMed: 31235753]

[61]. Liu Y, Xiong Z, Zhou W, Hua Y, Li C, Yao C, Percutaneous ultrasound-guided irreversible electroporation: A goat liver study, Oncol Lett, 4 (2012) 450–454. [PubMed: 24527063]

[62]. Brock RM, Beitel-White N, Coutermarsh-Ott S, Grider DJ, Lorenzo MF, Ringel-Scaia VM, Manuchehrabadi N, Martin RCG, Davalos RV, Allen IC, Patient Derived Xenografts Expand Human Primary Pancreatic Tumor Tissue Availability for ex vivo Irreversible Electroporation Testing, Front Oncol, 10 (2020) 843. [PubMed: 32528898]

[63]. Joshi RP, Schoenbach KH, Mechanism for membrane electroporation irreversibility under high-intensity, ultrashort electrical pulse conditions, Phys Rev E Stat Nonlin Soft Matter Phys, 66 (2002) 052901. [PubMed: 12513540]

[64]. Bao S, Wu Q, McLendon RE, Hao Y, Shi Q, Hjelmeland AB, Dewhirst MW, Bigner DD, Rich JN, Glioma stem cells promote radioresistance by preferential activation of the DNA damage response, Nature, 444 (2006) 756–760. [PubMed: 17051156]

[65]. Hoskin PJ, Crow J, Ford HT, The influence of extent and local management on the outcome of radiotherapy for brain metastases, Int J Radiat Oncol Biol Phys, 19 (1990) 111–115. [PubMed: 2116386]

[66]. Mintz AP, Cairncross JG, Treatment of a single brain metastasis: the role of radiation following surgical resection, JAMA, 280 (1998) 1527–1529. [PubMed: 9809735]

[67]. Patchell RA, Tibbs PA, Regine WF, Dempsey RJ, Mohiuddin M, Kryscio RJ, Markesbery WR, Foon KA, Young B, Postoperative radiotherapy in the treatment of single metastases to the brain: a randomized trial, JAMA, 280 (1998) 1485–1489. [PubMed: 9809728]

[68]. Vera-Tizatl CE, Talamas-Rohana P, Vera-Hernandez A, Leija-Salas L, Rodriguez-Cuevas SA, Chavez-Munguia B, Vera-Tizatl AL, Cell morphology impact on the set-up of electroporation protocols for in-suspension and adhered breast cancer cells, Electromagn Biol Med, 39 (2020) 323–339. [PubMed: 32762310]

[69]. Ciobanu F, Golzio M, Kovacs E, Teissie J, Control by Low Levels of Calcium of Mammalian Cell Membrane Electropermeabilization, J Membr Biol, 251 (2018) 221–228. [PubMed: 28823021]

[70]. Dermol J, Pakhomova ON, Pakhomov AG, Miklavcic D, Cell Electrosensitization Exists Only in Certain Electroporation Buffers, PLoS One, 11 (2016) e0159434. [PubMed: 27454174]

Highlights

- H-FIRE induces dose dependent permeability, apoptosis, and metabolic dysfunction.
- Select H-FIRE doses permit tumor cell damage recovery, allowing for proliferation.
- Higher H-FIRE doses suppress tumor cell damage recovery, inhibiting proliferation.

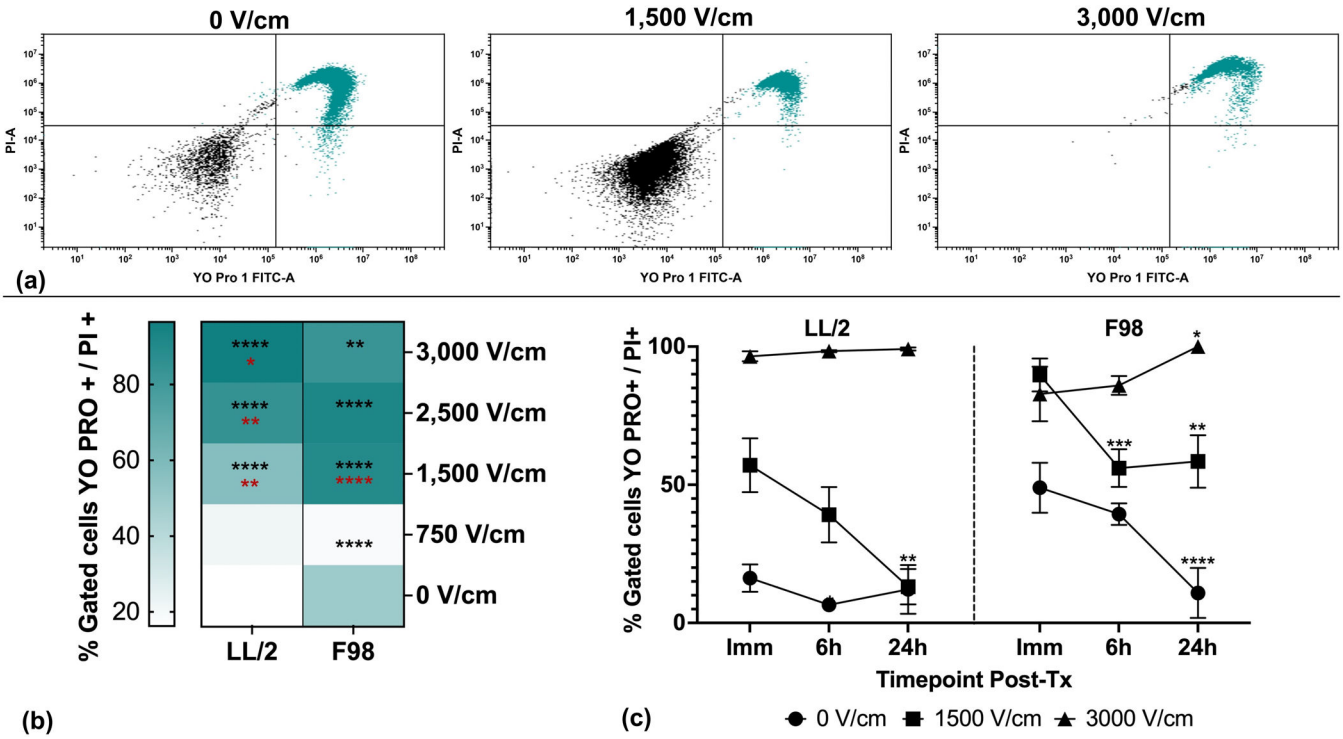

Figure 1. H-FIRE induces dose-dependent irreversible and recoverable tumor cell membrane permeability.

Suspensions of 1×10^6 cancer cells were treated with a single *in vitro* H-FIRE treatment protocol using escalating electric fields. Cells were stained and analyzed by flow cytometry immediately, 6h, and 24h post-treatment. YO-PRO®-1 and PI exclusion dye staining was used to quantify membrane permeability. **(a)** Representative flow cytometry dot plots and gating of LL/2 cells treated with 0, 1,500, and 3,000 V/cm H-FIRE showing immediate post-treatment YO-PRO®-1 and PI permeabiliy (green dots, right upper and lower quandrants). **(b)** Tumor cell membrane permeability (YO-PRO®-1 and PI double-positive cells) for all treatment levels for the immediate post-treatment timepoint. Percentages of cells permeabilized are presented as mean. Significant differences are shown between each treatment level and the sham group with black stars. Statistically significant differences are shown between each treatment level and the immediately preceding treatment level with red stars. **(c)** Temporal profiles of tumor cell permeability for select treatment levels that resulted in significant recovery of membrane permeability by 24 hours post-treatment (1,500 V/cm), no recovery (3,000 V/cm), and sham. Data are presented as mean ± SD. Significant differences between timepoints are noted compared to immediate post-treatment timepoint within each treatment level. Statistical analysis using a two-way ANOVA (Mixed Effects). ns $p \geq 0.05$, * $p < 0.05$, ** $p < 0.01$,*** $p < 0.001$, **** $p \leq 0.0001$. $n \geq 3$ for all groups.

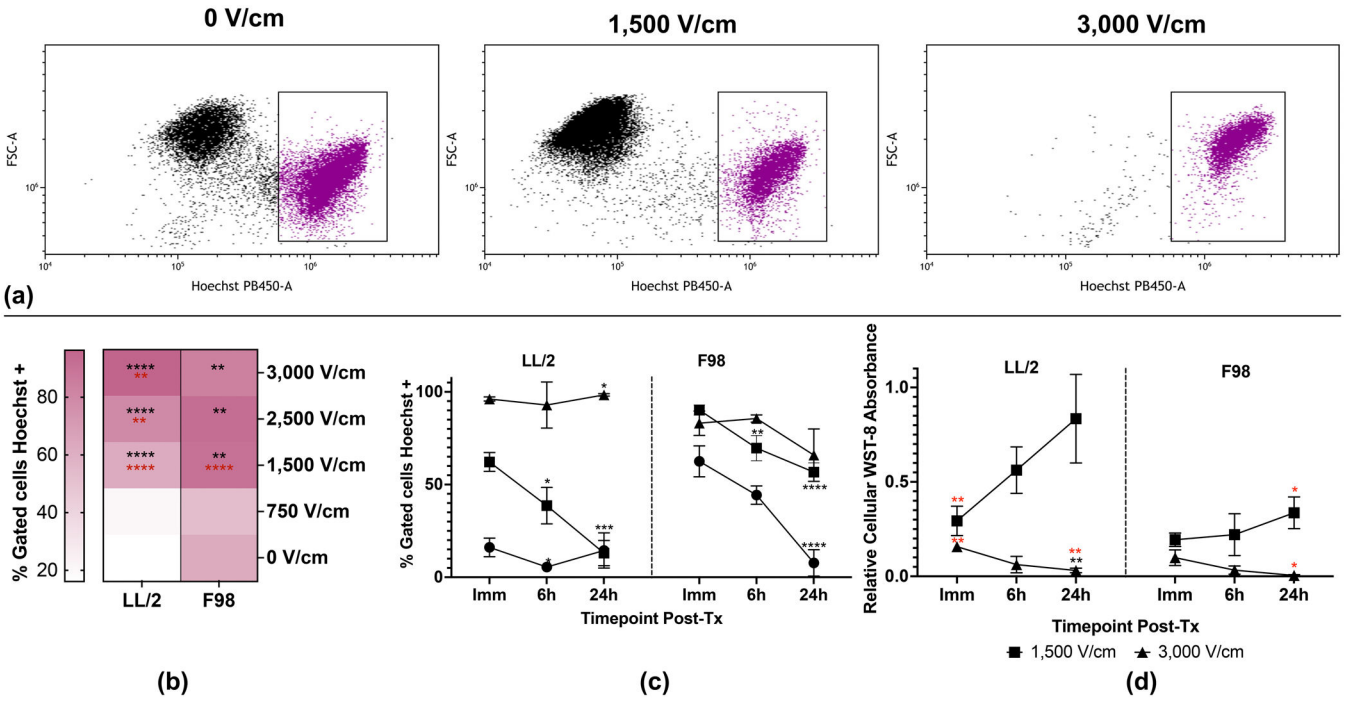

Figure 2. H-FIRE induces dose-dependent irreversible and recoverable tumor cell viability.

Suspensions of 1×10^6 cancer cells were treated with a single *in vitro* H-FIRE treatment protocol at 0, 1,500, 3,000 V/cm. For analysis of chromatin condensation, cells were stained with Hoechst-33342 and analyzed by flow cytometry immediately, 6h, and 24h post-treatment. For quantification of metabolic viability, cells were treated and plated to be analyzed immediately, 6h, and 24h post-treatment. **(a)** Representative flow cytometry dot plots and gating of LL/2 cells treated with 0, 1,500, and 3,000 V/cm H-FIRE showing immediate post-treatment Hoechst staining (purple dots). **(b)** Tumor cell chromatin condensation for all treatment levels at the immediate post-treatment timepoint. Data are presented as mean percentage of positive cells. Statistically significant differences are shown between each treatment level and the sham group in black. Statistically significant differences are shown between each treatment level and the immediately preceding treatment level in red. **(c)** Temporal profiles of tumor cell chromatin condensation for select treatment levels that resulted in significant recovery of membrane permeability by 24 hours post-treatment (1,500 V/cm), no recovery (3,000 V/cm), and sham. Data are presented as mean ± SD. Significant differences between timepoints are noted compared to immediate post-treatment timepoint within each treatment level in black. **(d)** Temporal profiles of WST-8 absorbance for select treatment levels that resulted in significant recovery of membrane permeability by 24 hours post-treatment (1,500 V/cm) and no recovery (3,000 V/cm) normalized to sham. Data are presented as mean ± SD. Significant differences between timepoints compared to immediate post-treatment within the same electric field are noted in black. Significant differences between electric fields compared to sham at the same timepoint are noted in red. Statistical analysis using a two-way ANOVA (Mixed-effects). ns $p \geq 0.05$, * $p < 0.05$, ** $p < 0.01$, *** $p < 0.001$, **** $p \leq 0.0001$. $n \geq 3$ for all groups.

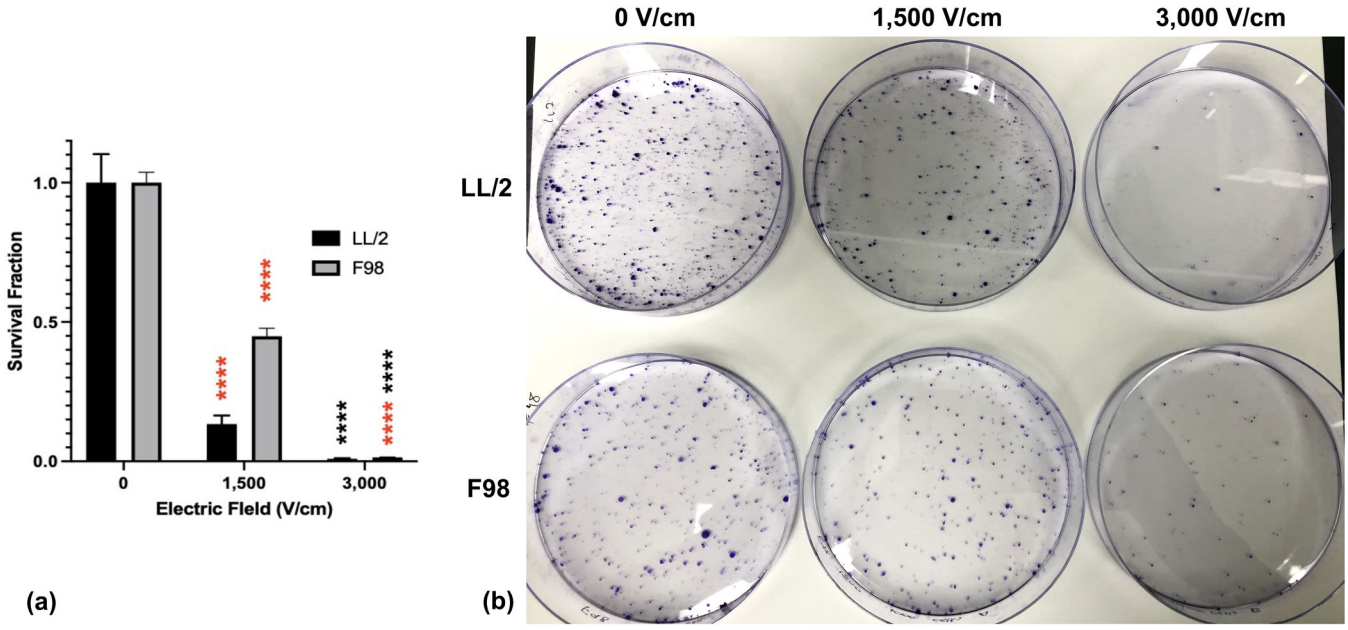

Figure 3. Tumor cells treated with damage recovery-permitting doses of H-FIRE maintain proliferative capacity.

Suspensions of 1×10^6 cancer cells were treated with a single *in vitro* H-FIRE treatment protocol at 0, 1,500, 3,000 V/cm and seeded in culture dishes at predetermined densities. Cells were incubated with growth media for 8 days and observed for colony formation. Colonies were stained with crystal violet to visualize and quantify colony formation and proliferative capacity. **a)** Survival fractions of tumor cell lines treated with varying doses of H-FIRE normalized to sham. Data are presentated as mean ± SD. Significant differences are noted between sequential electric fields in red and compared with sham in black. Statistical analysis using one-way ANOVA. ns $p \geq 0.05$, * $p< 0.05$, ** $p < 0.01$, *** $p < 0.001$, **** $p \leq 0.0001$. $n\geq3$ for all groups. **(b)** Clonogenic assay plates for LL/2 and F98 tumor cell lines treated with specified doses of H-FIRE. Purple dots indicate cancer colonies.